Optical localization in quasi-periodic multilayers

1998 J. Phys.: Condens. Matter 10 5839

(http://iopscience.iop.org/0953-8984/10/26/012)

J. Phys.: Condens. Matter **10** (1998) 5839–5849. Printed in the UK PII: S0953-8984(98)92652-2

Optical localization in quasi-periodic multilayers

M S Vasconcelos, E L Albuquerque† and A M Mariz
Departamento de Física, Universidade Federal do Rio Grande do Norte, Natal, RN 59072-970, Brazil

Received 17 March 1998

Abstract. We investigate the optical transmission spectra of quasi-periodic dielectric multilayer slabs arranged in a fashion that exhibits what has been called deterministic disorders. They can be of the so-called substitutional sequences type, and are characterized by the nature of their Fourier spectrum, which can be dense pure point (e.g. a Fibonacci sequence) or singular continuous (e.g. Thue–Morse and double-period sequences). The transmission coefficients are conveniently derived by using a theoretical model based on the transfer-matrix approach. A comparison between the oblique-incidence optical transmission spectrum and the normal-incidence one shows quite a different transmission behaviours over a particular range of frequency.

1. Introduction

Although the electronic properties of semiconductor superlattices and multi-quantum wells have attracted an enormous amount of attention in the last decade and more, considerably less effort has been made to investigate the optical properties of these artificial specimens. Special attention has been given to the so-called quasi-periodic structures, where two (or more) incommensurate periods are superposed, so that the resulting systems can be defined as intermediate between a periodic crystal and the random solid [1]. Experimental evidence of this new class of quasi-crystal has been given by Schechtman *et al* [2], and by Levine and Steinhardt [3]. Furthermore, it has been recognized that quasi-periodic systems could also lead to localized states (for a review, see [4, 5]).

Localization resulting from the electronic properties of a tight-binding Schrödinger equation has been studied in one dimension by several groups [6–9]. On the other hand, it has been shown [10–12] that propagation of light in quasi-periodic layered materials could provide an excellent tool for probing these localized states experimentally. The reason for that is that the localization phenomenon essentially arises due to the wave nature of the electronic states, and thus could be found in any wave phenomena. Also, a rather fascinating feature of these quasi-periodic structures is that they exhibit collective properties that are not shared by their constituents. Therefore, the long-range correlations induced by the construction of these systems are expected to be reflected in some way in their various spectra (electronic transmission, density of states, polaritons, Raman scattering etc), giving a novel description of disorder [13–15]. Indeed, theoretical transfer-matrix treatments [16, 17] show that these spectra are fractals.

On the other hand, the growth procedure of this kind of structure has become standard since the pioneering work of Merlin *et al* [18–20]. It involves defining two distinct building

† Author to whom any correspondence should be addressed; fax: (55)(84)2153791; e-mail: ela@dfte.ufrn.br.

blocks, each of them carrying the necessary physical information, and having them ordered in a desired manner (for instance, they can be described in terms of a series of generations that obey a particular recursion relation).

Recently, Gellermann *et al* [21] investigated experimentally the localization of a light wave which is *normally* incident on a dielectric multilayer following the Fibonacci sequence. They observed a scaling of the transmission coefficient with progression through the Fibonacci sequence at quarter-wavelength optical thickness. On the theoretical side, Liu [22] has investigated the *normal* propagation of light waves in dielectric multilayers following the Thue–Morse sequence. He also explored the localization properties of light in this quasi-periodic system.

It is the aim of this work to study the propagation of light waves in quasi-periodic structures composed of dielectric multilayers A and B stacked alternately following the Fibonacci, Thue–Morse and double-period sequences. Our aim is twofold. First we want to extend the previous work on this subject by considering the *oblique*-incidence case and introducing the aperiodic double-period system. The results are not merely a more complicated version of the normal-incidence case, since some interesting new aspects of the spectra are presented, like a striking difference between the transmission behaviours over a particular range of frequency. Second, we intend to give more insight into the optical spectra of these quasi-periodic structures, following our previous work on polaritons [23].

Let us briefly review the types of model considered in this work. First we recall the definition of a *substitutional sequence*. Take a finite set ξ (here $\xi = \{\mathrm{A}, \mathrm{B}\}$) called an *alphabet* and denote by ξ^* the set of all finitely long words that can be written in this alphabet. Now let ζ be a map from ξ to ξ^* by specifying that ζ acts on a word by substituting for each letter (e.g. A) of this word with its corresponding image $\zeta(\mathrm{A})$. A sequence is then called a *substitutional sequence* if it is a fixed point of ζ, i.e. if it remains invariant if each letter in the sequence is replaced by its image under ζ. As examples of substitutional sequences that have attracted the most attention in physics we have (all of them with $\xi = \{\mathrm{A}, \mathrm{B}\}$): (a) the Fibonacci sequence, where the substitution rules are $\mathrm{A} \rightarrow \zeta(\mathrm{A}) = \mathrm{AB}$, $\mathrm{B} \rightarrow \zeta(\mathrm{B}) = \mathrm{A}$; (b) the Thue–Morse sequence, with the rules $\mathrm{A} \rightarrow \zeta(\mathrm{A}) = \mathrm{AB}$, $\mathrm{B} \rightarrow \zeta(\mathrm{B}) = \mathrm{BA}$; (c) the double-period sequence, where $\mathrm{A} \rightarrow \zeta(\mathrm{A}) = \mathrm{AB}$, $\mathrm{B} \rightarrow \zeta(\mathrm{B}) = \mathrm{AA}$.

The plan of this work is as follows. In section 2, we present the method of calculation employed here, which is based on the transfer-matrix approach. Section 3 is devoted to the discussion of the transfer matrices for all of the quasi-periodic structures presented here. In section 4 we show the numerical results for these spectra, and give a discussion of their main features. The conclusions of this work are presented in section 5.

2. The transfer-matrix approach

Consider s-polarized (TE-wave) light of frequency ω incident from a transparent medium C at an arbitrary angle θ_{C} with respect to the normal direction of the layered system (see figure 1). The layered system is formed from an array of slabs of different materials (A or B). The reflectance and the transmittance coefficients are simply given by

$$R = \left|\frac{M_{21}}{M_{11}}\right|^2 \qquad T = \left|\frac{1}{M_{11}}\right|^2 \tag{1}$$

where M_{ij} $(i, j = 1, 2)$ are the elements of the optical transfer matrix $\mathbf{M}$, which links the coefficients of the electromagnetic fields in the region $z < 0$ to the coefficients of the electromagnetic fields in the region $z > L$, L being the size of the quasi-periodic structure.

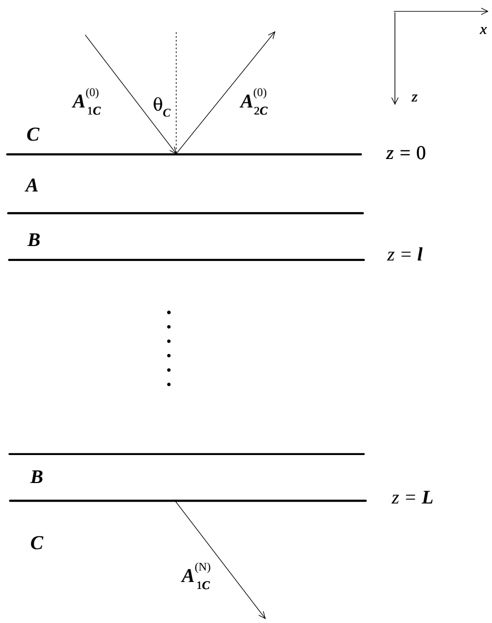

Figure 1. The geometry used in this paper ($l = a + b$).

Let us consider first, to illustrate our method, the optical transfer-matrix calculation for the periodic case which is characterized by having two alternating dielectric media A and B with thicknesses d_A and d_B, and refractive indexes n_A and n_B, respectively. It is surrounded by the transparent medium C with refractive index n_C (see figure 1). The transmission of an obliquely incident light wave across the interfaces $\alpha \to \beta$ (i.e., C $\to$ A, A $\to$ B, ..., B $\to$ C) is represented by the matrix

$$\mathsf{M}_{\alpha\beta} = \frac{1}{2}\begin{pmatrix} 1 + k_{z\beta}/k_{z\alpha} & 1 - k_{z\beta}/k_{z\alpha} \\ 1 - k_{z\beta}/k_{z\alpha} & 1 + k_{z\beta}/k_{z\alpha} \end{pmatrix} \tag{2}$$

with

$$k_{z\alpha} = [(n_\alpha \omega/c)^2 - k_x^2]^{1/2} \tag{3}$$

and

$$k_x = n_c(\omega/c)\sin(\theta_C). \tag{4}$$

The propagation of the light wave within one of the layers γ (γ = A or B) is characterized by the matrix

$$\mathsf{M}_\gamma = \begin{pmatrix} \exp(-\mathrm{i}k_{z\gamma}d_\gamma) & 0 \\ 0 & \exp(\mathrm{i}k_{z\gamma}d_\gamma) \end{pmatrix}. \tag{5}$$

We assume that, in each layer, the electrical field is given by

$$\begin{aligned} \boldsymbol{E}_\mathrm{j}^{(N)} &= (0, E_{y\mathrm{j}}^{(N)}, 0) \\ E_{y\mathrm{j}}^{(N)} &= [A_{1\mathrm{j}}^{(N)}\exp(-\mathrm{i}k_{z\mathrm{j}}z) + A_{2\mathrm{j}}^{(N)}\exp(\mathrm{i}k_{z\mathrm{j}}z)]\exp(\mathrm{i}k_x x - \mathrm{i}\omega t) \end{aligned} \tag{6}$$

where $A_{1\mathrm{j}}^{(N)}$ and $A_{2\mathrm{j}}^{(N)}$ (j = A or B; $N = 0, 1, 2, \ldots$) are the amplitudes.

Application of Maxwell's electromagnetic boundary conditions at the interface C/A, yields

$$\begin{pmatrix} A_{1\mathrm{C}}^{(0)} \\ A_{2\mathrm{C}}^{(0)} \end{pmatrix} = \mathbf{M}_{\mathrm{CA}} \begin{pmatrix} A_{1\mathrm{A}}^{(1)} \\ A_{2\mathrm{A}}^{(1)} \end{pmatrix}. \tag{7}$$

At the interface A/B, we find

$$\begin{pmatrix} A_{1\mathrm{A}}^{(1)} \\ A_{2\mathrm{A}}^{(1)} \end{pmatrix} = \mathbf{M}_{\mathrm{A}}\mathbf{M}_{\mathrm{AB}} \begin{pmatrix} A_{1\mathrm{B}}^{(3)} \\ A_{2\mathrm{B}}^{(3)} \end{pmatrix}. \tag{8}$$

Successive application of the matrices $\mathbf{M}$ along the finite structure gives

$$\begin{pmatrix} A_{1\mathrm{C}}^{(0)} \\ A_{2\mathrm{C}}^{(0)} \end{pmatrix} = \mathbf{M}_{\mathrm{CABAB\cdots BC}} \begin{pmatrix} A_{1\mathrm{C}}^{(N)} \\ 0 \end{pmatrix} \tag{9}$$

where

$$\mathbf{M}_{\mathrm{CABAB\cdots BC}} = \mathbf{M}_{\mathrm{CA}}\mathbf{M}_{\mathrm{A}}\mathbf{M}_{\mathrm{AB}}\mathbf{M}_{\mathrm{B}}\cdots\mathbf{M}_{\mathrm{B}}\mathbf{M}_{\mathrm{BC}}. \tag{10}$$

3. The quasi-periodic superlattices

We now intend to investigate the optical transfer matrices $\mathbf{M}$, given by (10) for the periodic case, for structures that exhibit deterministic disorders, i.e. Fibonacci, Thue–Morse and double-period structures.

A Fibonacci structure can be grown experimentally by juxtaposing the two building blocks A and B in such a way that the nth stage of the superlattice S_n is given interactively by the rule $S_n = S_{n-1}S_{n-2}$, for $n \geqslant 2$, with $S_0 = \mathrm{B}$ and $S_1 = \mathrm{A}$. The number of building blocks increases according to the Fibonacci number, $F_l = F_{l-1} + F_{l-2}$ (with $F_0 = F_1 = 1$), and the ratio between the number of building blocks A and the number of building blocks B in the sequence is equal to the golden mean number $\tau = (1+\sqrt{5})/2$.

The transfer matrix for the first Fibonacci sequence, $S_1 = \mathrm{A}$, is given by

$$\mathbf{M}_1 = \mathbf{M}_{\mathrm{CA}}\mathbf{T}_1\mathbf{M}_{\mathrm{AC}} \qquad \mathbf{T}_1 = \mathbf{M}_{\mathrm{A}}. \tag{11}$$

For the second, third, and fourth Fibonacci sequences, we have

$$\mathbf{M}_2 = \mathbf{M}_{\mathrm{CA}}\mathbf{T}_2\mathbf{M}_{\mathrm{BC}} \qquad \mathbf{T}_2 = \mathbf{M}_{\mathrm{A}}\mathbf{M}_{\mathrm{AB}}\mathbf{M}_{\mathrm{B}} \tag{12}$$

$$\mathbf{M}_3 = \mathbf{M}_{\mathrm{CA}}\mathbf{T}_3\mathbf{M}_{\mathrm{AC}} \qquad \mathbf{T}_3 = \mathbf{T}_2\mathbf{M}_{\mathrm{BA}}\mathbf{T}_1 \tag{13}$$

$$\mathbf{M}_4 = \mathbf{M}_{\mathrm{CA}}\mathbf{T}_4\mathbf{M}_{\mathrm{BC}} \qquad \mathbf{T}_4 = \mathbf{T}_3\mathbf{T}_2. \tag{14}$$

For any higher order ($n \geqslant 4$), we have

$$\mathbf{M}_n = \mathbf{M}_{\mathrm{CA}}\mathbf{T}_n\mathbf{M}_{\mathrm{BC}} \qquad \text{for } n \text{ even} \tag{15}$$

$$\mathbf{M}_n = \mathbf{M}_{\mathrm{CA}}\mathbf{T}_n\mathbf{M}_{\mathrm{AC}} \qquad \text{for } n \text{ odd} \tag{16}$$

with

$$\mathbf{T}_n = \mathbf{T}_{n-1}\mathbf{T}_{n-2} \qquad \text{for } n \text{ even} \tag{17}$$

$$\mathbf{T}_n = \mathbf{T}_{n-1}\mathbf{M}_{\mathrm{BA}}\mathbf{T}_{n-2} \qquad \text{for } n \text{ odd.} \tag{18}$$

The Thue–Morse sequence is defined by $S_n = S_{n-1}\ S_{n-1}^{+}$, $S_n^{+} = S_{n-1}^{+}S_{n-1}$ ($n \geqslant 1$), with $S_0 = \mathrm{A}$ and $S_0^{+} = \mathrm{B}$. The number of building blocks in this quasi-periodic system increases with 2^n, while the ratio of the number of building blocks A to the number of building blocks B is constant and equal to the unit.

The transfer matrices for the second, third and fourth Thue–Morse sequences are

$$\mathbf{M}_2 = \mathbf{M}_{\mathrm{CA}}\mathbf{M}_{\mathrm{A}}\mathbf{M}_{\mathrm{AB}}\mathbf{M}_{\mathrm{B}}\mathbf{M}_{\mathrm{B}}\mathbf{M}_{\mathrm{BA}}\mathbf{M}_{\mathrm{A}}\mathbf{M}_{\mathrm{AC}} = \mathbf{M}_{\mathrm{CA}}\mathbf{T}_{\alpha(2)}\mathbf{T}_{\beta(2)}\mathbf{M}_{\mathrm{AC}} \tag{19}$$

$$\mathbf{M}_3 = \mathbf{M}_{\mathrm{CA}}\mathbf{T}_{\alpha(3)}\mathbf{T}_{\beta(3)}\mathbf{M}_{\mathrm{BC}} \tag{20}$$

$$\mathbf{M}_4 = \mathbf{M}_{\mathrm{CA}}\mathbf{T}_{\alpha(4)}\mathbf{T}_{\beta(4)}\mathbf{M}_{\mathrm{BC}} \tag{21}$$

where

$$\mathbf{T}_{\alpha(2)} = \mathbf{M}_{\mathrm{A}}\mathbf{M}_{\mathrm{AB}}\mathbf{M}_{\mathrm{B}} \qquad \mathbf{T}_{\beta(2)} = \mathbf{M}_{\mathrm{B}}\mathbf{M}_{\mathrm{BA}}\mathbf{M}_{\mathrm{A}} \tag{22}$$

$$\mathbf{T}_{\alpha(3)} = \mathbf{T}_{\alpha(2)}\mathbf{T}_{\beta(2)} \qquad \mathbf{T}_{\beta(3)} = \mathbf{T}_{\beta(2)}\mathbf{T}_{\alpha(2)} \tag{23}$$

$$\mathbf{T}_{\alpha(4)} = \mathbf{T}_{\alpha(3)}\mathbf{M}_{\mathrm{AB}}\mathbf{T}_{\beta(3)} \qquad \mathbf{T}_{\beta(4)} = \mathbf{T}_{\beta(3)}\mathbf{M}_{\mathrm{BA}}\mathbf{T}_{\alpha(3)}. \tag{24}$$

For any higher order ($n \geqslant 4$), we have

$$\mathbf{M}_n = \mathbf{M}_{\mathrm{CA}}\mathbf{T}_{\alpha(n)}\mathbf{T}_{\beta(n)}\mathbf{M}_{\mathrm{AC}} \qquad \text{for } n \text{ even} \tag{25}$$

$$\mathbf{M}_n = \mathbf{M}_{\mathrm{CA}}\mathbf{T}_{\alpha(n)}\mathbf{T}_{\beta(n)}\mathbf{M}_{\mathrm{BC}} \qquad \text{for } n \text{ odd} \tag{26}$$

and

$$\mathbf{T}_{\alpha(n+1)} = \begin{cases} \mathbf{T}_{\alpha(n)}\mathbf{M}_{\mathrm{AB}}\mathbf{T}_{\beta(n)} & \text{for } n \text{ even} \\ \mathbf{T}_{\alpha(n)}\mathbf{T}_{\beta(n)} & \text{for } n \text{ odd} \end{cases} \tag{27}$$

$$\mathbf{T}_{\beta(n+1)} = \begin{cases} \mathbf{T}_{\beta(n)}\mathbf{M}_{\mathrm{BA}}\mathbf{T}_{\alpha(n)} & \text{for } n \text{ even} \\ \mathbf{T}_{\beta(n)}\mathbf{T}_{\alpha(n)} & \text{for } n \text{ odd.} \end{cases} \tag{28}$$

A similar rule holds for the double-period sequence, where the nth stage is given by $S_n = S_{n-1}S_{n-1}^+$, with $S_n^+ = S_{n-1}S_{n-1}$, $n \geqslant 1$. The number of building blocks for this sequence increase as in the Thue–Morse sequence, i.e., as 2^n, but the ratio between the number of building blocks α to the number of building blocks β is not constant; it tends to 2 when the number of the generation goes to infinity.

The transfer matrix for the first double-period sequence $S_1 = \mathrm{AB}$ is given by

$$\mathbf{M}_1 = \mathbf{M}_{\mathrm{CA}}\mathbf{T}_1\mathbf{M}_{\mathrm{BC}} \qquad \mathbf{T}_1 = \mathbf{M}_{\mathrm{A}}\mathbf{M}_{\mathrm{AB}}\mathbf{M}_{\mathrm{B}}. \tag{29}$$

For the second and third double-period sequences, we have

$$\mathbf{M}_2 = \mathbf{M}_{\mathrm{CA}}\mathbf{T}_2\mathbf{M}_{\mathrm{AC}} \qquad \mathbf{T}_2 = \mathbf{T}_1\mathbf{M}_{\mathrm{BA}}\mathbf{T}_0\mathbf{T}_0 \qquad \mathbf{T}_0 = \mathbf{M}_{\mathrm{A}} \tag{30}$$

$$\mathbf{M}_3 = \mathbf{M}_{\mathrm{CA}}\mathbf{T}_3\mathbf{M}_{\mathrm{BC}} \qquad \mathbf{T}_3 = \mathbf{T}_2\mathbf{T}_1\mathbf{M}_{\mathrm{BA}}\mathbf{T}_1. \tag{31}$$

For any higher order ($n \geqslant 3$),

$$\mathbf{M}_n = \mathbf{M}_{\mathrm{CA}}\mathbf{T}_n\mathbf{M}_{\mathrm{AC}} \qquad \text{for } n \text{ even} \tag{32}$$

$$\mathbf{M}_n = \mathbf{M}_{\mathrm{CA}}\mathbf{T}_n\mathbf{M}_{\mathrm{BC}} \qquad \text{for } n \text{ odd} \tag{33}$$

with

$$\mathbf{T}_n = \mathbf{T}_{n-1}\mathbf{M}_{\mathrm{BA}}\mathbf{T}_{n-2}\mathbf{T}_{n-2} \qquad \text{for } n \text{ even} \tag{34}$$

$$\mathbf{T}_n = \mathbf{T}_{n-1}\mathbf{T}_{n-2}\mathbf{M}_{\mathrm{BA}}\mathbf{T}_{n-2} \qquad \text{for } n \text{ odd.} \tag{35}$$

4. Numerical results

In this section we present some numerical results to illustrate the optical transmission spectra of some quasi-periodic structures. We consider the same physical parameters as were used in reference [21], i.e. those appropriate for silicon dioxide (A) and titanium dioxide (B); they are virtually free of absorption above 400 nm. Also we consider the individual layers as quarter-wave layers, for which the quasi-periodicity is expected to be more effective [24], with the central wavelength $\lambda_0 = 700$ nm. These conditions yield the physical thickness $d_J = 700/4n_J$ nm, J = A or B, such that $n_A d_A = n_B d_B$. Their dielectric constants around the central wavelength $\lambda_0 = 700$ nm are $n_A = 1.45$ and $n_B = 2.30$, respectively. We also consider medium C to be vacuum, and the phase shifts are given by

$$\delta_A = (\pi/2)\Omega\cos(\theta_A) \qquad \delta_B = (\pi/2)\Omega\cos(\theta_B) \tag{36}$$

where Ω is the reduced frequency $\omega/\omega_0 = \lambda_0/\lambda$.

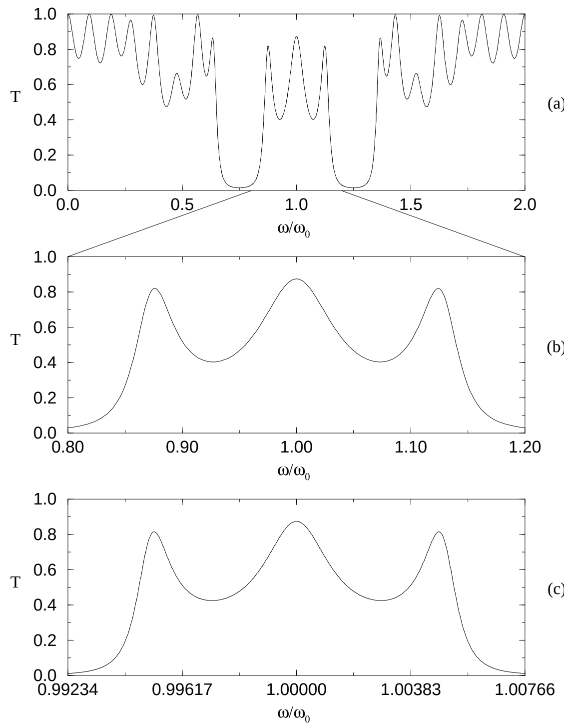

Figure 2. Normal-incidence transmission spectra: (a) Fibonacci's seventh generation (21 layers) as a function of the reduced frequency ω/ω_0; (b) as (a), but for the reduced range of frequency $0.80 \leqslant \omega/\omega_0 \leqslant 1.20$; (c) as (a), but for Fibonacci's thirteenth generation, with a different scale for ω/ω_0.

The optical transmission spectra for the seventh-generation (21-layer) quasi-periodic Fibonacci sequence, as a function of the reduced frequency ω/ω_0, are shown in figure 2(a) for the normal-incidence case, and in figure 3 for an angle of incidence $\theta_C = 80^\circ$. For the normal-incidence case, as expected, the transmission spectrum is symmetrical around the reduced frequency $\omega/\omega_0 = 1$ (which is of course the midgap frequency of a periodic quarter-wavelength multilayer), since in this case the phase shift $\delta_A = \delta_B = \pi/2$. The structure is quite transparent (the transmission coefficient is equal to 0.88) at this frequency. This condition implies that the layers A and B are equivalent from a wave point of view. Furthermore, the transmission spectrum has a scaling property with respect to the generation number of the Fibonacci sequence, within a symmetrical interval around $\omega/\omega_0 = 1$. To understand this scaling property, consider figure 2(b), which shows the optical transmission spectrum of figure 2(a) for the reduced range of frequency $0.80 \leqslant \omega/\omega_0 \leqslant 1.20$. This spectrum is similar, as shown in figure 2(c), to the one representing the thirteenth-generation

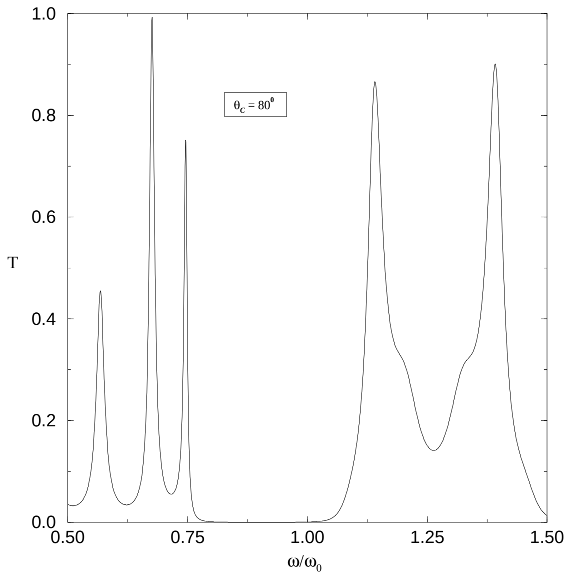

Figure 3. The oblique-incidence transmission spectrum ($\theta_{\rm C} = 80^\circ$) for Fibonacci's seventh generation as a function of the reduced frequency ω/ω_0. Observe the gap in the transmission coefficient for the approximate range $0.78 \leqslant \omega/\omega_0 \leqslant 1.05$.

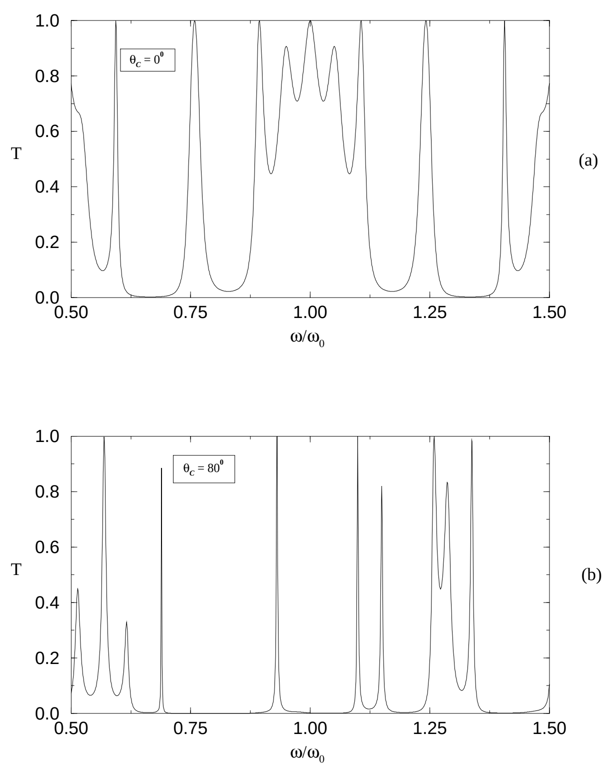

Figure 4. Optical transmission spectra for the Thue–Morse fifth generation (32 layers) as a function of the reduced frequency ω/ω_0: (a) normal incidence; (b) oblique incidence ($\theta_{\rm C} = 80^\circ$).

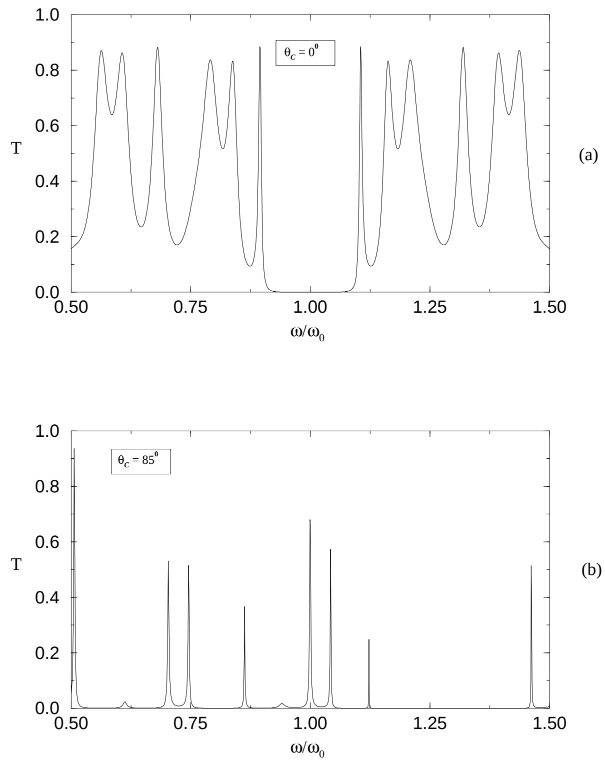

Figure 5. As figure 4, but for the double-period fifth generation (32 layers), and with $\theta_C = 85°$.

(144-layer) quasi-periodic Fibonacci sequence, for the range of frequency reduced by a scale factor equal to 26.11. Kohmoto *et al* [25] have found a similar result, but for an interval of three Fibonacci generations (six in our case), with a scale factor equal to 5.11 (5.11^2 in the present case). We have observed that this variation in the self-similarity properties is due only to the *substitution* of the medium surrounding the structure (vacuum in our case, medium A in Kohmoto's work). Therefore the sensitivity of the scaling factor to the surrounding medium indicates that the fractal behaviour of the spectra depends not only on the mathematical sequence (Fibonacci) which generates the quasi-periodic structure, but also on some constraints of the system (like medium C being vacuum).

For the oblique case ($\theta_C = 80°$), figure 3 shows a different situation. The transmission spectrum now shows a *large gap* for the frequency range $0.78 \leqslant \omega/\omega_0 \leqslant 1.05$. Also, the transmission spectrum is no longer symmetrical around $\omega/\omega_0 = 1$ and the structure is now completely opaque at this frequency. This fact indicates that the optical transmission is very sensitive to the angle of incidence.

The spectrum for the Thue–Morse quasi-periodic structure (fifth generation, totalling 32 layers) is shown in figure 4(a) for the normal-incidence case, and in figure 4(b) for an angle of incidence $\theta_C = 80°$. Instead of exhibiting the maximum transmission coefficient observed in figure 4(a), the structure, as in the Fibonacci case, is completely opaque at $\omega/\omega_0 = 1$. Also, we found a *large gap* for the frequency range $0.94 \leqslant \omega/\omega_0 \leqslant 1.09$, almost symmetrically distributed around $\omega/\omega_0 = 1$. This fact was first observed by Liu [22], using phenomenological variable parameters a and b to impose different phase shifts δ_A and δ_B, with the constraint that $a + b = 0.5$ imposed to ensure periodic quarter-wavelength

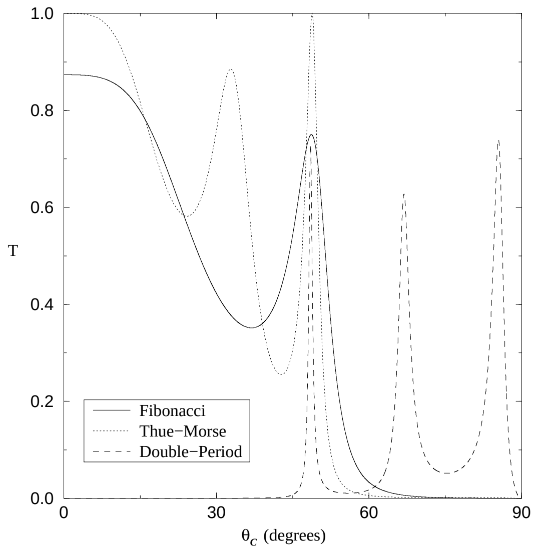

Figure 6. Transmission coefficients T at $\omega/\omega_0 = 1$ as a function of the angle of incidence θ_C for the Fibonacci (full line), Thue–Morse (dotted line) and double-period (dashed line) quasi-periodic structures. Observe the difference in their behaviours when we change the value of the angle of incidence from $\theta_C = 0$.

multilayers. Here we complement his observation, taking into account just the oblique-transmission spectrum. We have observed also that the spectra produced by changing the angle of incidence cannot be reproduced by a simple change of the structural parameters, as was the case for the phenomenological variables a and b used by Liu [22].

The normal-incidence optical transmission spectrum for the fifth-generation double-period quasi-periodic structure is shown in figure 5(a). The structure is symmetrically distributed around $\omega/\omega_0 = 1$, and is now completely *opaque* for the range of frequency $0.915 \leqslant \omega/\omega_0 \leqslant 1.085$. This is a surprising result, since, for the quasi-periodic structures obeying the Fibonacci and Thue–Morse sequences, we found a completely transparent region symmetrically distributed around $\omega/\omega_0 = 1$! For the oblique-incidence situation, with $\theta_C = 85°$, the transmission coefficient is equal to 0.68 at this frequency (compare with the completely opaque case found for the other sequences).

Figure 6 shows a comparison of the transmission behaviours of the Fibonacci (full line), Thue–Morse (dotted lines) and double-period (dashed lines) multilayers at $\omega/\omega_0 = 1$, for different angles of incidence. While the Fibonacci and Thue–Morse cases show an oscillatory behaviour of their transmission coefficients for angles of incidence in the range $0° \leqslant \theta_C \leqslant 75°$, with zero transmission coefficient otherwise, the double-period case shows this oscillatory behaviour for $40° \leqslant \theta_C \leqslant 90°$.

It is quite interesting, for the normal-incidence case and for a completely transparent frequency (with maximum transmission coefficient T) $\omega/\omega_0 = 2.0$ for the spectra of all of the quasi-periodic structures, that the electrical field distribution for each sequence follows its own structure. This can be seen from figure 7(a) for the Fibonacci case, figure 7(b) for the Thue–Morse situation and figure 7(c) for the double-period sequence. They have the same behaviours as those found in the electronic problem [26]. There is no counterpart for the oblique case.

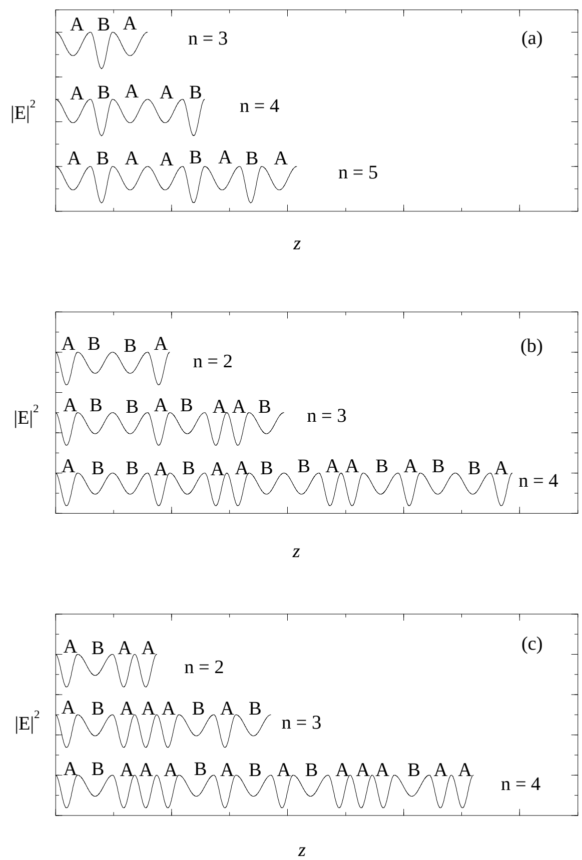

Figure 7. The normal-incidence electrical field distribution for a completely transparent frequency $\omega/\omega_0 = 2.0$, as a function of z (in nanometres), for the following structures: (a) the Fibonacci superlattice in the third, fourth and fifth generations; (b) the Thue–Morse superlattice in the second, third and fourth generations; (c) the double-period superlattice in the second, third and fourth generations.

5. Conclusions

In this work we have derived the recursion relations for the transfer-matrix elements in order to study the oblique propagation of light waves in Fibonacci, Thue–Morse and double-period multilayers. We have discussed the effects of oblique incidence on the transmission spectra of these quasi-periodic structures and found that they are very sensitive to the choice of the angle of incidence, with interesting different transmission behaviours. The opacity (or transparency) of the structure can be monitored using appropriate angles of incidence, and we believe that the information found here could help in experimental work on this subject. Note that it is the change of the angle of incidence that causes the modifications in the spectra. They cannot be obtained by just changing the structural parameters. We avoid discussing here the multi-fractal aspects of the spectra (with the exception of the Fibonacci case, where we have to do this in order to explain a qualitative difference between our spectra and those found by Kohmoto and co-workers), since they have already been studied in many investigations.

Acknowledgment

We thank the Brazilian Research Council CNPq for partial financial support.

References

[1] For a review, see, for example,
Steinhardt P J and Ostlund S 1987 *The Physics of Quasicrystals* (Singapore: World Scientific)
[2] Schechtman D, Blech I, Gratias D and Cahn J W 1984 *Phys. Rev. Lett.* **53** 1951
[3] Levine D and Steinhardt P J 1984 *Phys. Rev. Lett.* **53** 2477
[4] Lee P A and Ramakrishnan T V 1985 *Rev. Mod. Phys.* **57** 287
[5] Sokoloff J B 1985 *Phys. Rep.* **126** 189
[6] Ostlund S, Pandit R, Rand D, Schellnhuber H J and Siggia E D 1983 *Phys. Rev. Lett.* **50** 1873
[7] Kohmoto M and Oono Y 1984 *Phys. Lett.* **102A** 145
[8] Lu J P, Odagaki T and Birman J L 1986 *Phys. Rev.* B **33** 4809
[9] Nori F and Rodriguez J P 1984 *Phys. Rev.* B **34** 2207
[10] Kohmoto M and Banavar J R 1986 *Phys. Rev.* B **34** 563
Kohmoto M, Sutherland B and Tang C 1987 *Phys. Rev.* B **35** 1020
[11] Wang C and Barrio R A 1988 *Phys. Rev. Lett.* **61** 191
[12] Chow L and Guenther K H 1993 *J. Opt. Soc. Am.* A **10** 2231
[13] Luck J M 1989 *Phys. Rev.* B **39** 5834
[14] Axel F and Terauchi H 1991 *Phys. Rev. Lett.* **66** 2223
[15] Albuquerque E L and Cottam M G 1993 *Phys. Rep.* **233** 67
Albuquerque E L 1996 *Solid State Commun.* **99** 311
[16] Kolár M and Ali M K 1989 *Phys. Rev.* B **39** 426
Kolár M and Ali M K 1990 *Phys. Rev.* B **41** 7108
[17] Kolár M, Ali M K and Nori F 1991 *Phys. Rev.* B **43** 1034
[18] Merlin R, Bajema K, Clarke R, Juang F-Y and Bhattacharya P K 1985 *Phys. Rev. Lett.* **55** 1768
[19] Todd J, Merlin R, Clarke R, Mohanty K M and Axe J D 1986 *Phys. Rev. Lett.* **57** 1157
[20] Cheng Z, Savit R and Merlin R 1988 *Phys. Rev.* B **37** 4375
[21] Gellermann W, Kohmoto M, Sutherland B and Taylor P C 1994 *Phys. Rev. Lett.* **72** 633
[22] Liu Nian-hua 1997 *Phys. Rev.* B **55** 3543
[23] Vasconcelos M S and Albuquerque E L 1998 *Phys. Rev.* B **57** 2826
[24] Kono K, Nakada S, Narahara Y and Ootuka Y 1991 *J. Phys. Soc. Japan* **60** 368
[25] Kohmoto M, Sutherland B and Iguchi K 1987 *Phys. Rev. Lett.* **58** 2436
[26] Ryu C S, Oh G Y and Lee M H 1992 *Phys. Rev.* B **46** 5162
Ryu C S, Oh G Y and Lee M H 1993 *Phys. Rev.* B **48** 132